Вісник Астрономічної школи | Astronomical School's Report

ISSN 1607–2855

Том 8 • № 1 • 2012 С. 55 – 57

UDC 524.7

The structure of X-ray jet of 3C 273

A.V. Bogdan[1], **V.V. Marchenko**[2], **B.I. Hnatyk**[1]

[1]Astronomical Observatory of Kiev National University

[2]Astronomical Scientific Research Center, Taras Shevchenko National Pedagogical University of Chernihiv

The X-ray internal structure of extragalactic jets is analyzed. The Lucy-Richardson deconvolution algorithm is used to restore the image of X-ray sources. The analysis was done for Chandra observations of core-dominated quasar 3C 273. The transverse profiles are built for the jet knots.

СТРУКТУРА РЕНТГЕНІВСЬКОГО ДЖЕТУ КВАЗАРА 3C 273, Богдан А.В., Марченко В.В., Гнатик Б.І. — Досліджено внутрішню рентгенівську структуру позагалактичних джетів. Для відновлення рентгенівського зображення було використано алгоритм розгортки Люсі–Річардсона. Дослідження проведено для спостережень ядерно-домінантного квазара 3C 273 телескопом Чандра. Побудовано поперечні профілі для вузлів джету.

СТРУКТУРА РЕНТГЕНОВСКОГО ДЖЕТА КВАЗАРА 3C 273, Богдан А.В., Марченко В.В., Гнатык Б.И. — Исследована внутренняя рентгеновская структура внегалактических джетов. Для восстановления рентгеновского изображения было использовано алгоритм развертки Люси–Ричардсона. Исследование проведено для наблюдений ядерно-доминантного квазара 3C 273 телескопом Чандра. Построено поперечные профили для узлов джета.

Ключевые слова: квазары; джеты; рентгеновское излучение.

Key words: quasars; jets; X-ray emission.

1. INTRODUCTION

The active galactic nuclei (AGN) remain one of the most interesting and remarkable issues in modern astrophysics [1]. One of the manifestations of AGN activity is the existence of extragalactic jets that constitute the longest collimated structures in the Universe [2]. The detailed study of extragalactic jet structure in all wavelengths is important task for modeling the different astrophysical processes that take place in jet, for example the acceleration of cosmic rays up to the ultra high energies due to Fermi acceleration mechanisms [3], [4] and acceleration on the jet boundary [5].

2. OBSERVATIONAL DATA

We have used four Chandra observations of core-dominated quasar 3C 273 and its jet (ObsIDs: 4876, 4877, 4878, 4879) with total exposure time of 160 ks [6]. The X-ray data analysis was processed with CIAO 4.4 — a software package for Chandra interactive analysis of observations [7]. We have merged four observations for further analysis (ObsIDs: 4876, 4877, 4878, 4879) and have binned them with binning factor of 0.125 (it corresponds to bin size 0.0615″). The merged and binned image of jet is presented in Figure (1). Before the main analysis we reprocessed data using reprocessing script that makes all recommended data processing steps presented in the CIAO analysis threads. The pixel randomization was removed during reprocessing. We have not included energy-dependent sub-pixel event repositioning algorithm (EDSER) because the current version of SAOsac ray-trace simulator does not model the dither motion of the telescope so currently it's not possible to use EDSER in point spread function (PSF) model.

3. LUCY-RICHARDSON DECONVOLUTION ALGORITHM

Image of astronomical source observed from space can be mathematically described as a convolution of the intrinsic brightness distribution of the source with a blurring function, also known as a point spread function (PSF). Therefore one of the possibilities to restore the intrinsic source distribution from the observed data is to use some of deconvolution techniques.

In the present research we have used the Lucy-Richardson deconvolution algorithm that is implemented in CIAO 4.4 in "arestore" tool [8]. This algorithm requires the PSF image and we have used the modeled PSF generated by ChaRT and MARX – the programs for detailed ray-trace simulation [9, 10].

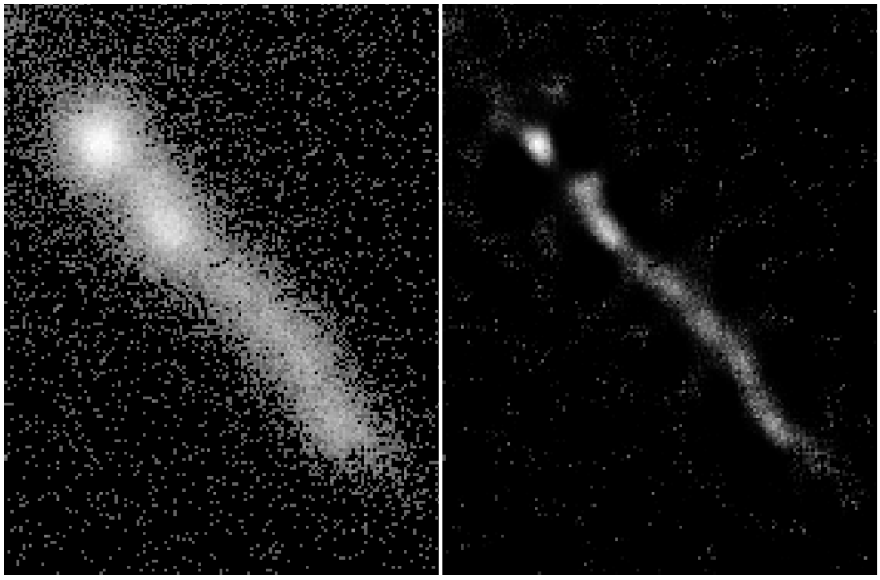

Fig. 1. The merged Chandra image of 3C 273 jet binned in $0.0615''$ bins (left) and restored image of 3C 273 jet using the Lucy-Richardson deconvolution algorithm with number of iteration $n = 120$ (right).

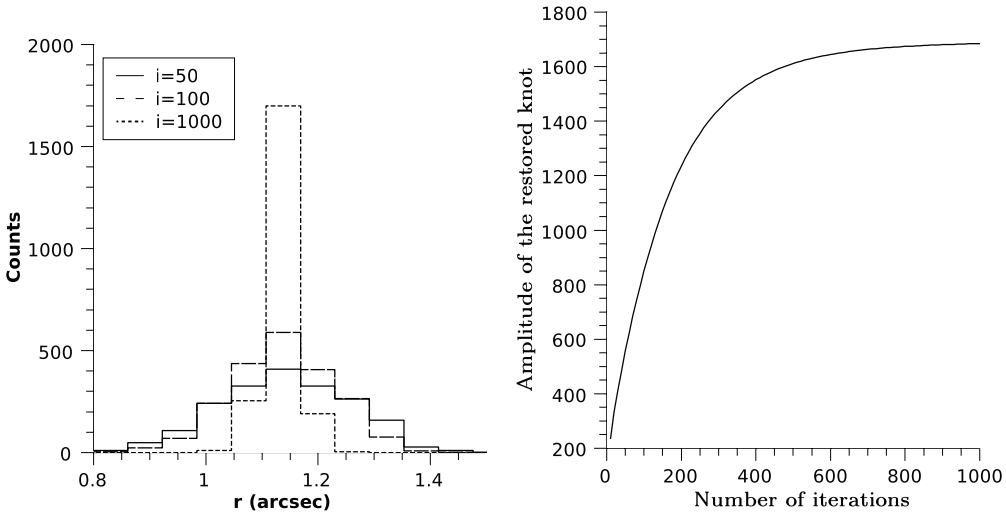

Fig. 2. Transverse knot profiles (left) and knot amplitude (right) for different number of iterations.

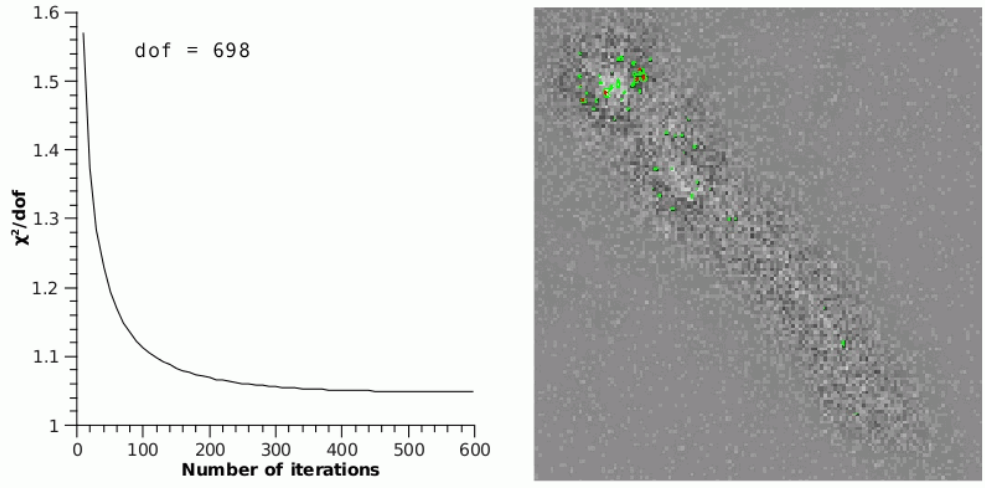

Fig. 3. χ^2 for different number of iterations (left) and residual map normalized by standard deviation (right).

4. RESULTS AND CONCLUSIONS

Taking into account the fact, that the Lucy-Richardson deconvolution method does not produce reliable convergence and uncertainty information, users should be very cautious in interpreting and evaluating the results of the deconvolution, especially when applied to faint and/or extended sources. Also it's noticeable, that the characteristics of restored image (width of knots, amplitude etc.) slightly vary for different number of iterations to perform, that is one of input parameters for Lucy-Richardson deconvolution algorithm (Fig. 2).

In order to ensure that the result of deconvolution is in good correspondence with observed data and to choose reasonable number of iterations we have decided to inspect it by comparing the restored image with observed data. For this we have constructed the model of data as a result of convolution of the restored image with PSF

$$M_i = S_i \circ P_i,$$

where M_i, S_i and P_i is the numbers of counts per bin i in model, restored image and PSF respectively. In order to estimate the optimal number of iterations we need to explore what number of iterations produces the physical model that describes the data in the best way. To figure it out we have used χ^2 statistic for different number of iterations

$$\chi^2 = \sum_i \frac{(N_i - M_i)^2}{\sigma_i^2},$$

where N_i is the total number of observed counts in bin i and σ_i is the error in bin i .

At the present research we take into account only statistical noise as an error. We assume that counts are sampled from the Poisson distribution with a mean value equals to total number of observed counts N_i in a bin. So the count standard deviation for a bin i can be taken as $\sigma_i = \sqrt{N_i}$. But when the average number of counts in the bin is small ($N_i < 5$), then we cannot assume that the Poisson distribution – from which the counts are sampled – has a nearly Gaussian shape. The standard deviation for such low-count case has been derived as $\sigma_i = 1 + \sqrt{N_i + 0.75}$ [11].

We have calculated χ^2 for different number of iterations and have shown that χ^2 decreases with the number of iterations. We have decided to choose the reasonable number of iteration reaching the $\chi^2 = 1.1$. It corresponds to number of iterations $n \approx 120$ (Figures 3 and 1).

Also to inspect the distribution of residuals between data N_i and model M_i across the image and to find the regions with significant deviations we have analyzed the residuals $N_i - M_i$. To analyze the residual in bin i one have to take into account that the significance of this residual depends on the error σ_i in this bin. Therefore we have normalized the residuals by standard deviation σ_i, namely $R_i = (N_i - M_i)/\sigma_i$ (Figure 3).

Acknowledgments. The authors acknowledge to Michal Ostrowski (Astronomical Observatory of Jagiellonian University, Poland), Lukasz Stawarz (Japan Aerospace Exploration Agency, Japan) and Dan Harris (Harvard-Smithsonian Center for Astrophysics, USA) for assistance and fruitful discussions.

1. *Comastri A., Brusa M.* Extragalactic X-ray surveys: AGN physics and evolution // Astronomische Nachrichten. — 2008. — **329**. — P.122.
2. *Harris D.E., Massaro F., Cheung C.C.* The Classification of Extragalactic X-ray Jets // AIP Conference Proceedings. — 2010. — **1248**. — P. 355–358.
3. *Ostrowski M.* Acceleration of ultra-high energy cosmic ray particles in relativistic jets in extragalactic radio sources // Astronomy and Astrophysics. — 1998. — **335**. — P. 134–144.
4. *Kataoka J., et al.* The X-Ray Jet in Centaurus A: Clues to the Jet Structure and Particle Acceleration // The Astrophysical Journal. — 2006. — **641**. — P. 158–168.
5. *Ostrowski M.* Cosmic Ray Acceleration at Relativistic Shocks // Journal of Physical Studies. — 2002. — **6**. — P. 393–400.
6. *Jester S., et al.* New Chandra Observations of the Jet in 3C 273. I. Softer X-Ray than Radio Spectra and the X-Ray Emission Mechanism // The Astrophysical Journal. — 2006. — **648**. — P. 900–909.
7. *Fruscione A., et al.* CIAO: Chandra's Data Analysis System // Chandra Newsletter. — 2007. — **14**. — P. 36.
8. CIAO 4.4: http://cxc.harvard.edu/ciao/ahelp/arestore.html
9. *Carter C., et al.* ChaRT: The Chandra Ray Tracer, ADASS XII // ASP Conference Series. — 2003. — **295**. — P.477.
10. *Wise M.W., Huenemoerder D.P., Davis J.E.* Simulated AXAF Observations with MARX, Astronomical Data Analysis Software and Systems VI // A.S.P. Conference Series. 1997. — **125**. — P. 477.
11. *Gehrels N.* Confidence limits for small numbers of events in astrophysical data // Astrophysical Journal. — 1986. — **303**. — P. 336–346.

Received 30.10.2012